Article

Curcumin nanocrystal/pH-responsive polyelectrolyte multilayer core-shell nanoparticles for inflammation-targeted alleviation of ulcerative colitis

Murtada A. Oshi, Juho Lee, Muhammad Naeem, Nurhasni Hasan, Jihyun Kim, Hak Jin Kim, Eun Hee Lee, Yunjin Jung, and Jin-Wook Yoo

Biomacromolecules, **Just Accepted Manuscript** • DOI: 10.1021/acs.biomac.0c00589 • Publication Date (Web): 23 Jul 2020

Curcumin Nanocrystal/pH-Responsive Polyelectrolyte Multilayer Core-Shell Nanoparticles for Inflammation-Targeted Alleviation of Ulcerative Colitis

Murtada A. Oshi,[a] Juho Lee,[a] Muhammad Naeem,[a] Nurhasni Hasan,[a] Jihyun Kim,[a,b] Hak Jin Kim,[c] Eun Hee Lee,[d] Yunjin Jung,[a] and Jin-Wook Yoo[a]

[a] College of Pharmacy, Pusan National University, Busan, South Korea

[b] Department of Cogno-Mechatronics Engineering, College of Nanoscience & Nanotechnology, Pusan National University, Busan, South Korea

[c] Department of Radiology, Pusan National University Hospital, Pusan National University School of Medicine, Busan, South Korea

[d] College of Pharmacy, Korea University, Sejong, South Korea

ABSTRACT

In this study, we developed oral core-shell nanoparticles composed of curcumin nanocrystals in the core and chitosan/alginate multilayers in the shell for inflammation-targeted alleviation of ulcerative colitis (UC). Release rate of curcumin from the core-shell

nanoparticles was low at a pH mimicking the stomach and small intestine, whereas it was higher at a pH mimicking the colon. Further, bio-distribution studies in the gastrointestinal tract of mice showed that distribution of nanoparticles was significantly higher in colon than that in stomach and small intestine. Quantitative analysis of drug in colonic tissues and confocal imagining of colons revealed preferential accumulation of nanoparticles in inflamed tissues than that in healthy tissues. *In vivo* anti-inflammatory studies revealed that nanoparticles exhibit enhanced efficacy in alleviating inflammation-related symptoms in mouse colitis model. The results suggest that the core-shell nanoparticles presented here can be exploited as efficient colon-targeted drug delivery systems for UC therapy.

KEYWORDS: Chitosan, core-shell nanoparticles, curcumin nanocrystals, inflammation-targeted delivery, sodium alginate, ulcerative colitis

INTRODUCTION

Ulcerative colitis (UC) is a chronic, recurrent inflammatory disease of the innermost lining of the colon and rectum.[1, 2] Delivery of orally administered drugs to the colon is highly desirable in UC therapy, as it can result in low systemic toxicity and high efficacy of the drug.[3, 4] However, delivery of the drugs to the colon is challenging owing to the physiological and anatomical barriers associated with the gastrointestinal tract (GIT), such as degradation of the drug in acidic pH conditions prevalent in the lumen, presence of digestive enzymes, and physical adsorption by the mucosa.[5, 6] To address these issues, various types of nanocarrier-based drug delivery systems, such as polymeric nanoparticles,[7, 8] lipid nanoparticles,[9] silica nanoparticles,[10] liposomes,[11, 12]

nanoparticles in microparticles,[13] and nanogels[14] have been developed. However, low drug loading capacity and excipient-associated side effects are intrinsic limitations associated with these drug delivery systems. In addition, the fabrication cost of these systems is high.[15-17] Therefore, to overcome these limitations, new types of nanocarrier-based drug delivery systems are urgently needed.

One promising approach to address these limitations is to fabricate drugs in nanocrystal forms.[18, 19] Unlike the other types of nanocarrier-based systems, the core of the drug nanocrystals is entirely composed of the drug (~100 %) and stabilized using lesser amounts of excipient.[20-22] In addition, the excipient-associated side effects can be minimized *in vivo* by using nanocrystals as drug delivery systems. Thus, there is a substantial interest in the targeted delivery of the drug nanocrystals to the colon. This will result in high doses of the drug molecule at the site of disease, thus enhancing the therapeutic efficacy of the drugs. However, none of the fabricated drug nanocrystals have been used till date for colon-targeted delivery to treat diseases such as UC. One of the reasons for this is that the drug nanocrystals rapidly dissolve in the upper GIT following oral administration before reaching the targeted colonic regions due to their small particle size.[20] In addition, the drug nanocrystals are reported to exhibit poor adhesion and accumulation in cells and tissues.[23] Designing in-core-shell nanoparticles is one of the many strategies being investigated for lowering the rate of drug dissolution from nanoparticles.[24] Core-shell nanoparticles are a class of nanostructured materials comprising an inner core structure surrounded by external shells prepared from different polymeric materials.[25] This unique structure has generated special interest in using core-shell nanoparticles as carriers in the field of drug delivery. The key features of core-shell nanoparticles include high drug loading efficiency and controlled drug release.[24, 26]

In this study, we have developed curcumin nanocrystals (CUNCs) surrounded by chitosan (CH), sodium alginate (AG), and cellulose acetate phthalate (CAP) polyelectrolyte multilayer core-shell nanoparticles for colon-targeted therapy of UC. With this system, our goal is to deliver CUNCs to the colon and ensuring that they are not dissolved in the upper GIT, thereby resulting in a high availability of the drug in the colon for therapeutic activity. Further, we aimed at enhancing the accumulation of CUNCs into inflamed colonic tissues by exploiting the surface-charge reversing property of the multilayers surrounding the nanoparticles. In this study, the shell of the core-shell nanoparticles was prepared using polyelectrolytes capable of changing the surface charge of the shell from negative in the upper GIT to positive in the colon depending on pH variation. In our earlier study, we had demonstrated that a pH-triggered surface charge-reversal of nanoparticles promoted their adhesion and accumulation in the inflamed colonic tissues by enabling their interaction with negatively charged-mucins in the mucosa during UC therapy.[9]

MATERIALS AND METHODS

Materials

Curcumin was purchased from Sigma-Aldrich (St. Louis, MO, USA). CH (Mw 50,000 - 190,000 Da, viscosity 20 - 30 cP and deacetylation $\geq$ 75 %), AG (Mw 80,000 - 120,000 Da, viscosity $\geq$ 2000 cP and mannuronate/guluronate ratio 1.56), and CAP (Mw 2534.12, hydroxyl content 3.6 % and acetyl content 39.8 %) were obtained from Sigma-Aldrich (St. Louis, MO, USA). Dextran sodium sulfate (DSS) was obtained from MP Biomedicals (Irvine, CA, USA). Mouse interleukin-6 (IL-6) DuoSet® ELISA KIT was purchased from R&D System (Minneapolis,

MN, USA). Tumor necrosis factor- α (TNF-α) ELISA MAX® was purchased from BioLegend Inc (San Diego, CA, USA). Anti-rabbit IgG labeled with Alexa Flour 568 was purchased from Thermo Fisher Scientific (Waltham, USA). Anti-F4/80 antibody and polyclonal anti-myeloperoxidase were obtained from Abcam (Cambridge, UK). Alexa Flour 488-conjugated goat anti-mouse IgG antibody was purchased from Jackson ImmunoResearch Inc (West Grove, PA, USA). All other reagents and solvents were of the highest analytical grade commercially available.

Preparation of core-shell nanoparticles

CUNCs/CH, AG and CAP multilayer core-shell nanoparticles ($CAP_1AG_4CH_5$@CUNCs) were prepared by ultrasound-assisted antisolvent crystallization and layer by layer (LBL)-coating techniques (Figure 1A).[27, 28] Briefly, curcumin (2 mg/mL in 60 % ethanol) was added to CH (2 mg/mL in 0.1 M acetic acid, pH 5) and sonicated (150 W/cm2) at 4°C for 30 min. The resulting suspension was centrifuged at 20,000 × *g* for 20 min and washed thrice with 0.05 % NaCl to obtain chitosan-coated curcumin nanocrystals (CH_1@CUNCs). CH_1@CUNCs were then re-suspended in 20 mL of AG solution (2 mg/mL in water, pH 5) and gently shaken for 20 min to allow AG coating on the surfaces. The resulting suspension was centrifuged at 20,000 × *g* for 20 min and washed thrice with 0.05 % NaCl. The coating was then continued using CH and AG alternately until the desired number of CH/AG multilayer was obtained (AG_4CH_5@CUNCs). Finally, AG_4CH_5@CUNCs were incubated in CAP solution (2 mg/mL, pH 6) for 20 min and washed thrice with 0.05 % NaCl to obtain $CAP_1AG_4CH_5$@CUNCs.

Characterization of core-shell nanoparticles

The particle shape of $CAP_1AG_4CH_5$@CUNCs was characterized by scanning electron microscopy (SEM) (SUPRA 40 VP ZEISS Ltd, USA). A drop of diluted suspension of nanoparticles was placed on a carbon tape, air dried at room temperature (25 °C) in a desiccator and imaged at an accelerating voltage of 15 kV after coating with gold-palladium alloy. The core-shell structure of $CAP_1AG_4CH_5$@CUNCs was characterized by transmission electron microscope (TEM) (H7600 Hitachi, Japan) in accordance with a previously described procedure.[29]

Dynamic light scattering (DLS) was used for measuring the particle size, polydispersity index (PDI) and zeta potential of $CAP_1AG_4CH_5$@CUNCs by Malvern Zetasizer Nano ZS90, (Malvern Panalytical, UK). Three independent samples of nanoparticles were diluted in water, dispersed well, and measured at a fixed angle of 137° at 25 °C.

Differential scanning calorimetry (DSC) was performed using PerkinElmer DSC instrument (Waltham, USA) to examine the crystalline state of curcumin in CH_1@CUNCs and $CAP_1AG_4CH_5$@CUNCs. Five milligrams of curcumin powder, CH_1@CUNCs and $CAP_1AG_4CH_5$@CUNCs were accurately weighed and heated at a temperature ranging from 0 - 300 °C with a heating rate of 10 °C/min.

pH-dependent drug release study

To study the effect of pH on drug release rate, $CAP_1AG_4CH_5$@CUNCs were studied using a gradually pH-changing buffer solution that mimicked the pH variation in the human GIT.[30] Briefly, 22.5 mg of nanoparticles was suspended in 50 mL of 0.1 N hydrochloric acid (pH 1.2) and agitated (60 rpm) at 37 °C for 2 h. The pH of the buffer was then increased to 4.5 by adding a powder

mixture containing 2.28 g of tris(hydroxymethyl) aminomethane and 1.77 g of anhydrous sodium acetate and the experiment was performed for 3 h. The pH of the buffer was further increased to 7.2 by adding the same powder mixture again and the study was continued till completion, i.e., 24 h. At predetermined time intervals, 500 µL of the sample was collected from the solution and centrifuged at 45,000 × g at 4 °C for 30 min. Then, the drug content in the supernatant was analyzed by high-performance liquid chromatography (HPLC)[31] and the pellet was redispersed in the release buffer solution with 500 µL of fresh medium to avoid the loss of nanoparticles. The HPLC system (Shimadzu, Tokyo, Japan) used was equipped with an autosampler processor, SPD-20A ultraviolet (UV) detector, and C18 column (5 µm, 250 mm × 4.6 mm). The mobile phase consisting of a mixture of methanol: H_2O (containing 3.6 % glacial acetic acid) (73:27, v/v) was pumped at a flow rate of 1 mL/min. The sample injection volume was set at 20 µL and the UV detector was set at 306 nm. The retention time was 7.5 min at 25 °C.

pH-dependent charge-reversing study

The surface charge-reversing property of $CAP_1AG_4CH_5$@CUNCs was studied by measuring their zeta-potential at different pH values following previously described procedure.[9] The nanoparticles were added to the buffers with different pH values, similar to the varying pH conditions in the human GIT (stomach 1.2, small intestine 4.5 and colon 7.2) and incubated in a shaking water bath (60 rpm) at 37 °C for predetermined times. Then, the nanoparticles were collected by centrifugation at 20,000 × *g* for 20 min and washed thrice with distilled water (20,000 × *g* for 20 min). Finally, they were re-suspended in distilled water and surface charge was measured using DLS method (Malvern Zetasizer Nano ZS90, Malvern Panalytical, UK).

Bio-distribution of core-shell nanoparticles in mice GIT

The bio-distribution of CH_1@CUNCs and core-shell nanoparticles in the different segments of the GIT in colitis-induced mice was studied. Briefly, mice were randomly divided into the following four groups (n = 6 mice per group): control (no drug treatment), CH_1@CUNCs, AG_4CH_5@CUNCs (core-shell nanoparticles without CAP layer), and $CAP_1AG_4CH_5$@CUNCs. Nanoparticle suspensions were prepared and orally administered to mice (curcumin concentration of 50 mg/kg of body weight) for 6 h or 12 h. At the end of each experiment, the mice were euthanized and the GIT segments, including luminal contents were excised. The drug contents from different segments, such as stomach, small intestine and colon were then analyzed using HPLC.[32]

The bio-distribution of CH_1@CUNCs and core-shell nanoparticles in mice GIT was also studied using an *in vivo* imaging system (IVIS) (FOBS; Nanoscience, South Korea). For fluorescent imaging of mice GIT, IR-780 dye was used as fluorescent probe after assembling with curcumin in core-shell nanoparticles.[33] Briefly, mice were divided into 4 experimental groups (n = 6 in each group). The control group did not receive any drug, while the other groups were orally administered with CH_1@CUNCs, AG_5CH_5@CUNCs, or $CAP_1AG_4CH_5$@CUNCs at a curcumin dose of 0.5 mg/kg. After 6 h or 12 h of administration, the mice were euthanized and the entire GIT was excised for *ex vivo* fluorescence imaging.

Accumulation of core-shell nanoparticles into inflamed colonic tissues

The accumulation of CH_1@CUNCs and core-shell nanoparticles in the inflamed colonic tissues of mice was analyzed quantitatively and the results were compared to that in healthy colons.[9] Briefly, mice were divided into 4 groups (n = 6 in each group). The control group did not receive drug, while the other groups were orally administered with CH_1@CUNCs, AG_5CH_5@CUNCs or $CAP_1AG_4CH_5$@CUNCs at a curcumin dose of 50 μg per mice. After 12 h of administration, mice were euthanized, colons were excised, and samples from healthy and inflamed colons were freeze-dried. Thirty milligrams of healthy and inflamed colon samples were used to extract curcumin with one milliliter of ethanol and the drug concentrations in the samples were quantified by HPLC.[34]

To further investigate the accumulation of CH_1@CUNCs and core-shell nanoparticles in inflamed colonic tissues of mice, confocal laser scanning microscopy (CLMS) (Olympus FV10i, Tokyo, Japan) was used. For confocal imaging of the colonic tissues of mice, curcumin was used as fluorescence probe.[30] Samples from inflamed colons were fixed in 4 % paraldehyde prepared in 10 % sucrose for 12 h at 4 ˚C. The colon samples were then embedded in Tissue-Tek® O.C.T. compound (Sakura, Netherlands), cut into 5 μm sections, and visualized.

Animal model and treatments

All animal studies in this work were in compliance with the regulations of Pusan National University, Busan, South Korea (PNU-IACUC, approval number: PNU-2018-2038). Imprinting control region (ICR) mice (30 - 35 g body weight) were housed at the university animal center at 25 ± 3 °C under a 12 h light/dark cycle for 7 days before the induction of colitis. Colitis was induced in mice by supplementing 2.5 % (w/v) DSS in drinking water for 7 days. Age and sex-matched mice were given access to tap water and considered as healthy control group. After the

induction of colitis, DSS water was replaced with normal tap water and drug treatment was started. Mice were divided into five experimental groups: healthy control, colitis control, CH_1@CUNCs-treated, AG_5CH_5@CUNCs-treated and $CAP_1AG_4CH_5$@CUNCs-treated. The mice in drug-treated groups received an equal dose of a curcumin (15 mg/kg) in the form of suspension by oral gavage for 7 days. Mice in healthy and colitis groups did not receive any curcumin.

Macroscopic grading of colitis

The macroscopic assessment of colitis was performed based on disease activity index (DAI), colon length and spleen weight of mice. DAI was monitored blindly, starting from first day of induction of colitis until the last day of treatment, and includes a sum of 3 parameters: body weight, stool consistency, and rectal bleeding.[35] Briefly, the loss in body weight was scored in a four point scale: no weight loss was assigned a score of 0, 1 – 5 % weight loss was assigned a score of 1, 5 – 10 % of weight loss was assigned a score of 2, 10 - 20% weight loss was assigned a score of 3, and > 20 % weight loss was assigned a score of 4. Similar scaling was used for stool consistency: well-formed pellets stool was assigned 0, semi-formed stool was assigned a score of 2, and liquid stool was assigned a score of 4 points. Similarly, for rectal bleeding: no blood was assigned a core of 0, positive finding was assigned a score of 2, and gross bleeding was assigned a score of 4. All mice were euthanized by CO_2 asphyxiation after 24 h of last drug treatment and the colon and spleen were carefully removed. Resected colon and spleen were rinsed with cold phosphate buffer and colon length and spleen weight were measured as gross clinical features for assessing the colitis severity.[36]

Histological analysis of colitis

To evaluate the therapeutic efficacy of core-shell nanoparticles on the severity of colitis, histological analysis of mice colon tissues was performed using Hematoxylin-Eosin (H&E) staining. The mice colon samples were fixed in neutral buffer with 10 % formalin and embedded in wax. The embedded colons were then cut into 5 µm-thick sections using microtome (Reichert, Munich, Germany), stained with H&E, and scanned using light microscopy (Zeiss, Axioskop, Germany). The severity of colitis in each colonic section was assessed by evaluating mucosal features, such as epithelium damage, mucosal edema, and infiltration of inflammatory cells into mucosa using a blinded approach.[37]

Neutrophil and macrophage infiltration into mucosa

Immunofluorescence was performed on the colon samples for detecting neutrophil and macrophage infiltration in mucosa.[38] Formalin-fixed paraffin-embedded colon samples were cut into 5 µm-thick sections using microtome (Reichert, Munich, Germany) and incubated with blocking solution (Tris buffer with 2 % BSA). Further, to detect neutrophil infiltration, the tissue sections were incubated overnight with polyclonal anti-myeloperoxidase (1:200 dilution) at 4 °C, followed by incubation with the secondary antibody Alexa Flour 488-conjugated goat anti-mouse IgG (1:200 dilution) for 1 h at 25 °C. Similarly, for detecting macrophage infiltration, the tissue sections were incubated overnight with primary anti-F4/80 antibody (1:500 dilution) at 4°C, followed by incubation with anti-rabbit IgG labeled with Alexa Flour 568 (1:200 dilution) secondary antibody for 3 h at 25°C. Finally, the colonic sections were counterstained with 5 µg/mL

of 4',6-diamidino-2-phenylindole (DAPI) and analyzed using confocal microscopy (Olympus FV10i, Tokyo, Japan).

Measurement of MPO activity and pro-inflammatory cytokine levels

MPO activity in the colon tissues was measured by following a previously described method.[39] Briefly, 50 mg of the tissue sample was homogenized in 2 mL of ice-cold 50 mM phosphate buffer (pH 6.0) containing 0.5% hexa-decyltrimethyl ammonium bromide at 30 Hz and 4 ˚C for 4 min. The homogenate was then centrifuged at 13,400 × *g* for 6 min at 4°C. The supernatant was then collected and added to 0.0167% o-dianisidine hydrochloride (o-dianisidine) solution and 0.0005% hydrogen peroxide (H_2O_2), and the change in absorbance was measured at 450 nm at intervals of 30 s. The o-dianisidine solution was prepared by dissolving 16.7 mg of o-dianisidine in 90 mL of distilled water and 10 mL of 50 mM phosphate buffer. MPO activity was calculated as a unit of MPO per mg of tissue. One unit of MPO was defined as the amount needed to degrade 1 μmol H_2O_2 per min.

The concentration of interleukin-6 (IL-6) and tumor necrosis factor (TNF-α) were quantified in the colons samples according to an established method described by Kim et al.[39] Briefly, 50 mg of the colon tissue samples were homogenized in 1 mL of protease inhibitor cocktail and lysis buffer solution (10 mL of 1 M tris-hydrochloric acid (pH = 8.0), 6 mL of 5 M sodium chloride and 2 mL of Triton X-100 in 182 mL of sterilized distilled water) for 5 min at 30 Hz. The homogenate was centrifuged at 3300 × *g* for 5 min at 4 °C and the supernatant was used to quantify IL-6 and TNF-α by a sandwich-type enzyme-linked immunosorbent assay as per the supplier's instructions.

RESULTS

Preparation and characterization of core-shell nanoparticles

In this study, CH_1@CUNCs were prepared using the anti-solvent crystallization technique (Figure 1A). The curcumin solution was added to the CH solution to form CH_1@CUNCs under sonication. As curcumin is highly hydrophobic and tends to self-aggregate into large clumps in solution,[40] an ultrasonic powder was used to prevent particle aggregation and to obtain desired particle size. CH_1@CUNCs with a particle size of 380 nm and PDI value of 0.09 were successfully prepared (Table 1).

Table 1. Physicochemical characteristics of core-shell nanoparticles

Formulation	Particle size (nm)	PDI	Zeta potential (mV)	Drug loading (%)
CH_1@CUNCs	380 ± 90	0.09 ± 0.02	+ 34 ± 7	94 ± 7
AG_5CH_5@CUNCs	420 ± 17	0.29 ± 0.04	- 36 ± 2	90 ± 4
$CAP_1AG_4CH_5$@CUNCs	421 ± 14	0.21 ± 0.01	- 47 ± 3	91 ± 3

Note: results are expressed as mean ± SD (n = 3).

To prepare $CAP_1AG_4CH_5$@CUNCs, CH_1@CUNCs were coated with multiple layers of CH and AG followed by CAP using an LBL-coating technique. To confirm the coating of CH, AG, and CAP on CH_1@CUNCs surface, zeta potential of the resulted particles was measured during every coating step. Successful coating of each polyelectrolyte layer was confirmed based on the change in charge between positive and negative during every coating step, as shown in Figure 1B.

Analysis of CH_1@CUNCs and $CAP_1AG_4CH_5$@CUNCs using SEM confirmed the cubic shape of nanoparticles (Figure 2A and C). Moreover, TEM was used to analyze the core-shell structure of CH_1@CUNCs and $CAP_1AG_4CH_5$@CUNCs (Figure 2B and D, respectively). As shown in Figure 2D, the high contrast dark black region indicates the CUNCs core, whereas, the light darker part surrounding the core confirms the presence of CH/AG/CAP multilayer shell. The diameter of the curcumin core was approximately 270 - 280 nm, while the thickness of the CH/AG/CAP multilayer shells was approximately 50 - 100 nm (Figure 2D). In general, it has been reported that the core-shell nanoparticles with thick shell have the advantage of achieving a sustained drug release from their inner cores.[41]

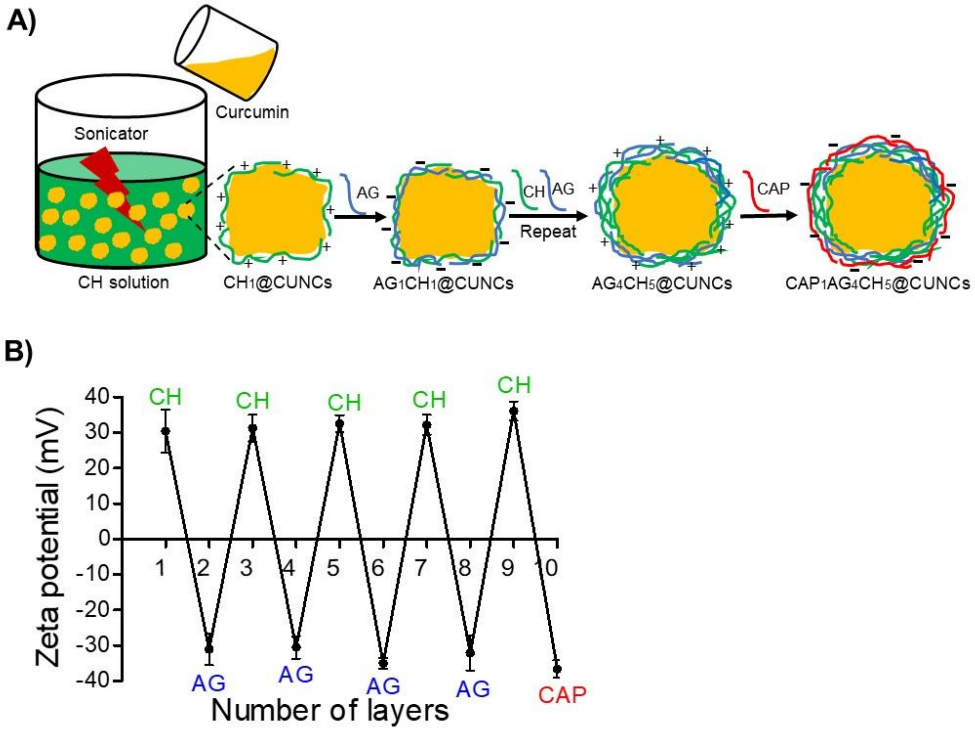

Figure 1. Preparation of core-shell nanoparticles and their zeta potential at different stages. (A) Schematic diagram of $CAP_1AG_4CH_5$@CUNCs preparation using ultrasound-assisted antisolvent

crystallization and LBL-coating techniques. (B) Change in zeta-potential of CH_1@CUNCs as a function of the number of CH, AG, and CAP layers during the preparation of $CAP_1AG_4CH_5$@CUNCs. Data are represented as means ± SD (n = 6).

$CAP_1AG_4CH_5$@CUNCs with an average diameter of 421 ± 14 nm and PDI of 0.21 ± 0.01 were successfully prepared in this study (Table 1). The small PDI value indicated the narrow particle size distribution of $CAP_1AG_4CH_5$@CUNCs. To examine the crystalline state of curcumin in the core, DSC analysis was performed for CH_1@CUNCs and $CAP_1AG_4CH_5$@CUNCs and was compared with that of curcumin powder. $CAP_1AG_4CH_5$@CUNCs showed endotherm peaks with a melting point at ~ 175 °C, which coincided with that of free curcumin and CH_1@CUNCs (Figure 2E), indicating that the crystalline state of CH_1@CUNCs was not affected by the LBL-coating process.

$CAP_1AG_4CH_5$@CUNCs showed a high drug loading efficiency with up to 90 % for curcumin. Although, the drug loading efficiency of $CAP_1AG_4CH_5$@CUNCs was found to be slightly lesser than that of CH_1@CUNCs, it was insignificant (Table 1). Further, it should be noted that high drug content is one of the important advantages of drug delivery systems prepared by the LBL-coating technique.[42]

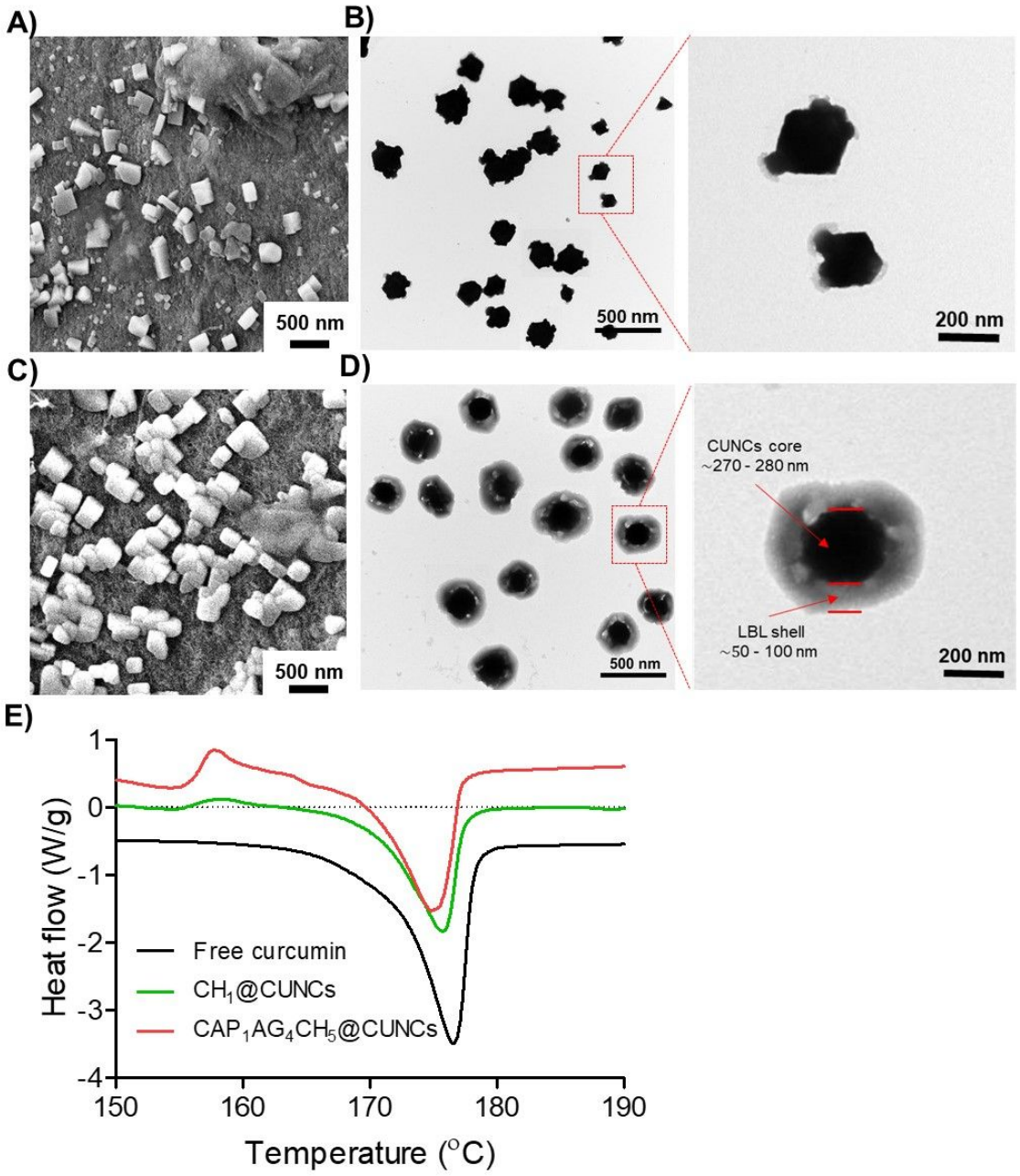

Figure 2. Physical characterization of core-shell nanoparticles. SEM and TEM images of CH_1@CUNCs (A and B, respectively) and $CAP_1AG_4CH_5$@CUNCs (C and D, respectively), indicating the core-shell structure of nanoparticle. (E) DSC peak of free curcumin, CH_1@CUNCs and $CAP_1AG_4CH_5$@CUNCs.

pH-dependent drug release and charge-reversal studies

To evaluate the effect of shell thickness on pH-dependent drug release, core-shell nanoparticles with different shell thickness (different number of CH/AG/CAP multilayers) were prepared (Table 1 and Table S1). Drug release from core-shell nanoparticles was shown to be reduced in the first 5 h at pH 1.2 and 4.5 by increasing the number of CH/AG/CAP multilayers. Approximately, 20 - 80 % of total curcumin was released from core-shell nanoparticles depending on the number of CH/AG/CAP multilayers (Figure 3A). However, core-shell nanoparticles with less than 10 multilayers of CH/AG/CAP, such as $CAP_1AG_1CH_2$@CUNCs, $CAP_1AG_2CH_3$@CUNCs, and $CAP_1AG_3CH_4$@CUNCs showed burst drug release at pH 1.2 and 4.5. Further, core-shell nanoparticles with 10 CH/AG/CAP multilayers, $CAP_1AG_4CH_5$@CUNCs, showed ~ 3-fold lesser curcumin release than others at pH 1.2 and 4.5. Total curcumin released from $CAP_1AG_4CH_5$@CUNCs at pH 1.2 and 4.5 was ~ 20 % (Figure 3B). However, by increasing the pH of the buffer to 7.2, $CAP_1AG_4CH_5$@CUNCs showed sustained drug release with the remaining curcumin payload released in ~ 9 h (Figure 3A). These results indicate that the shell thickness of 50 - 100 nm having 10 CH/AG/CAP layers ($CAP_1AG_4CH_5$@CUNCs) is responsible for the controlled drug release from the nanoparticle cores. This hypothesis was partially supported by the release profile of AG_5CH_5@CUNCs, which exhibited burst drug release at pH 1.2 and 4.5. Approximately 80 % of the total drug payload of AG_5CH_5@CUNCs was released in the first 5 h of the study at pH 1.2 and 4.5 (Figure 3B).

The pH-dependent charge reversal property of the core-shell nanoparticles was studied by measuring their zeta-potential in buffer solutions with different pH (Figure 3C). $CAP_1AG_4CH_5$@CUNCs exhibited negative surface charge of - 37 ± 4 mV and - 36 ± 5 mV at pH

1.2 and 4.5, respectively, owing to the presence of CAP outer layer. In contrast, in a buffer with pH 7.2, $CAP_1AG_4CH_5$@CUNCs exhibited a positive surface charge of 34 ± 4 mV, because of the dissolution of CAP outer layer and exposure of the CH layer beneath.

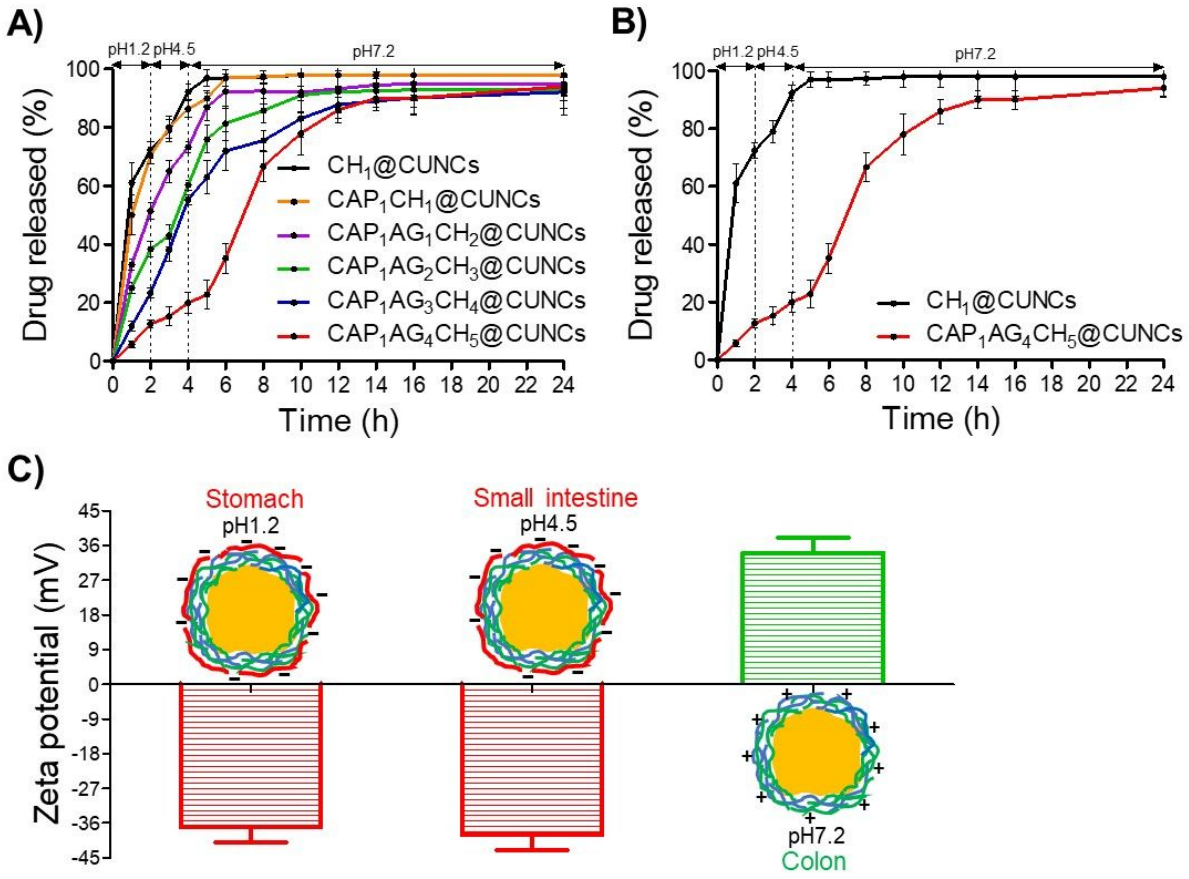

Figure 3. Drug release and charge reversal properties of the nanoparticles based on pH variation. (A) pH-dependent drug release from core-shell nanoparticles with shells containing different numbers of CH/AG/CAP multilayers. (B) pH-dependent drug release from AG_5CH_5@CUNCs and $CAP_1AG_4CH_5$@CUNCs. (C) pH-dependent surface charge reversal of $CAP_1AG_4CH_5$@CUNCs. Data are represented as means ± SD (n = 6).

Bio-distribution of core-shell nanoparticles in mice GIT

Figure 4A and B show the maximum recovery of curcumin from the different GI tract segments after 6 and 12 h post-administration of CH_1@CUNCs and core-shell nanoparticles to mice. For AG_5CH_5@CUNCs, ~ 8 % of curcumin was recovered from the small intestine after 6 h post-administration, whereas trace amounts of curcumin were detected in stomach as well as colon (Figure 4A). After 12 h post-administration of AG_5CH_5@CUNCs, negligible amounts of curcumin were detected in the stomach, small intestine and colon. The reason for the small amounts of curcumin recovered after 6 h and 12 h post-administration of AG_5CH_5@ CUNCs is presumably due to the systemic absorption of curcumin in the stomach and small intestine before reaching the colon. For $CAP_1AG_4CH_5$@CUNCs, maximum recovery of ~ 45 % and ~ 40 % of curcumin was achieved from the colon after 6 and 12 h post-administration, respectively (Figure 4B). The drug recovery from $CAP_1AG_4CH_5$@CUNCs in case of the small intestine was found to be ~ 35 % and ~ 7 % 6 and 12 h post-administration to mice, respectively, and negligible amounts were found in the stomach (Figure 4B). It was worth to mention that no curcumin was recovered from the stomach, small intestine and colon after 6 and 12 h post-administration of CH_1@CUNCs to mice.

Figure 4C shows representative IVIS images demonstrating the bio-distribution of CH_1@CUNCs and core-shell nanoparticles in different GIT segments after 6 and 12 h post-administration. CH_1@CUNCs showed no significant fluorescent signal in the GIT segments after 6 and 12 h post-administration to mice. For AG_5CH_5@CUNCs, weak fluorescence signals were detected in the stomach, small intestine, and cecum (not colon) after 6 h post-administration, which completely disappeared after 12 h (Figure 4C). These results proved that AG_5CH_5@CUNCs had dissolved in the stomach and small intestine before reaching the colon. In contrast,

$CAP_1AG_4CH_5$@CUNCs showed high fluorescence signals in the small intestine and colon after 6 h, with signals being detected in the colon after 12 h post-administration (Figure 4C). These results indicated that $CAP_1AG_4CH_5$@CUNCs are more efficiently distributed in the colon as compared to CH_1@CUNCs and AG_5CH_5@CUNCs.

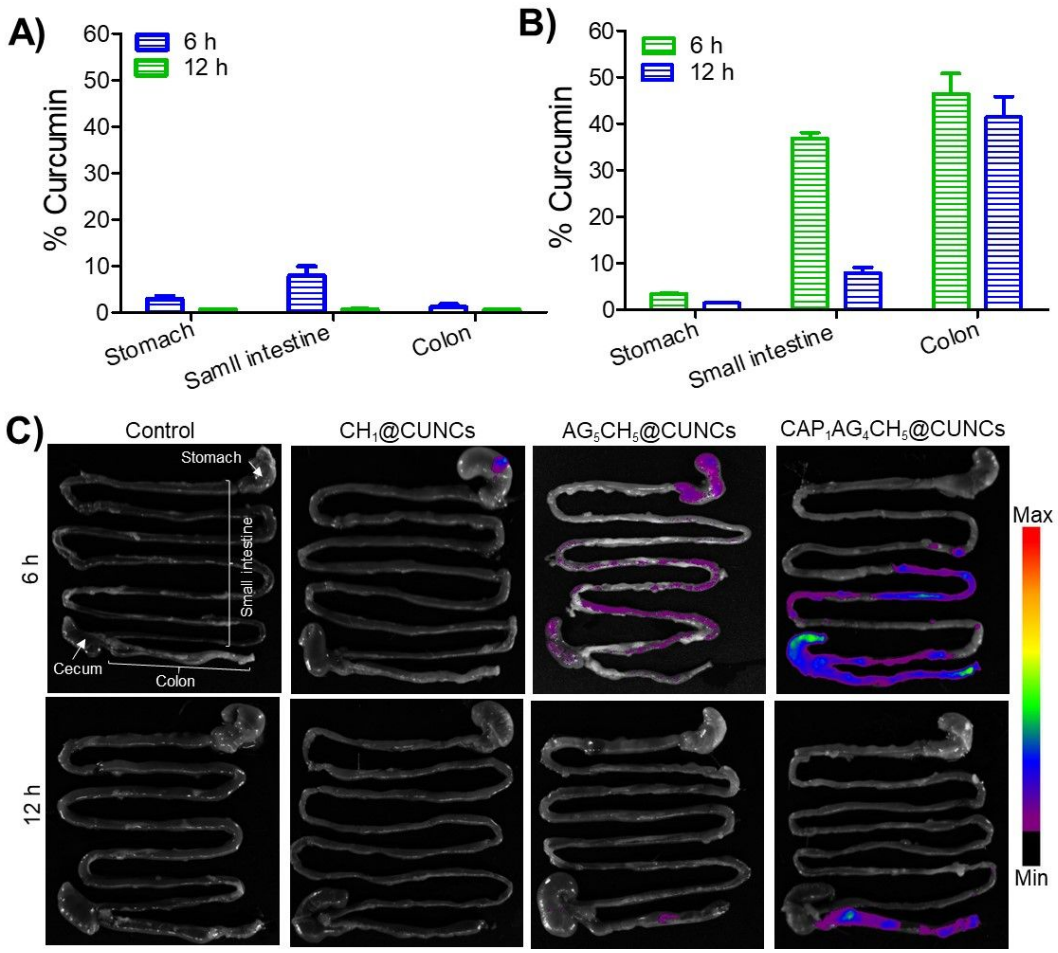

Figure 4. Bio-distribution of CH_1@CUNCs and core-shell nanoparticles in different segments of mice GIT. Quantitative analysis indicating bio-distribution of AG_5CH_5@CUNCs (A) and $CAP_1AG_4CH_5$@CUNCs (B) in different mice GIT segments 6 and 12 h post- administration. (C)

IVIS images of mice GIT showing the bio-distribution of CH_1@CUNCs, AG_5CH_5@CUNCs and $CAP_1AG_4CH_5$@CUNCs 6 and 12 h post-administration to mice. Data are represented as means ± SD (n = 6).

Accumulation of core-shell nanoparticles in the inflamed colonic tissues

The accumulation of CH_1@CUNCs and core-shell nanoparticles in the inflamed colons was analyzed quantitatively and compared to that of healthy colons (Figure 5A). For mice administered with $CAP_1AG_4CH_5$@CUNCs, significant amounts of curcumin were recovered from the healthy and inflamed colonic tissues. However, the concentration of the curcumin recovered from the inflamed tissues (3500 ng/g tissue) was significantly higher ($p < 0.001$) than that from healthy colon (798 ng/g tissue) (Figure 5A). These results indicate that $CAP_1AG_4CH_5$@CUNCs accumulate more effectively in the inflamed colonic tissues than in healthy colonic tissues, presumably *via* the charge-reversal properties of core-shell nanoparticles. As expected, no curcumin was recovered from both healthy and inflamed colonic tissues obtained from mice administered with CH_1@CUNCs or AG_5CH_5@CUNCs.

We further investigated the accumulation of CH_1@CUNCs and core-shell nanoparticles in the inflamed colonic tissues of colitis using a confocal microscopy. Figure 5B shows confocal images of colons demonstrating the accumulation of CH_1@CUNCs and core-shell nanoparticles in the inflamed colonic tissues of colitis mice. No fluorescence signal was detected in the colonic tissue of mice with CH_1@CUNCs, indicating that few nanoparticles are accumulated in the colonic tissues. For mice with AG_5CH_5@CUNCs, the signal was too weak to distinguish it from the colonic tissue autofluorescence (Figure 5B). In contrast, the inflamed colonic tissues of the

mice administered with $CAP_1AG_4CH_5$@CUNCs showed stronger fluorescence signals than those treated with CH_1@CUNCs or AG_5CH_5@CUNCs. At 12 h post-administration of mice, $CAP_1AG_4CH_5$@CUNCs highly accumulated in the inflamed colonic tissues (Figure 5B). These results were consistent with the curcumin quantitative results and further indicated that $CAP_1AG_4CH_5$@CUNCs were more preferentially accumulated in the inflamed colonic tissues of mice than CH_1@CUNCs and AG_5CH_5@CUNCs (Figure 5C).

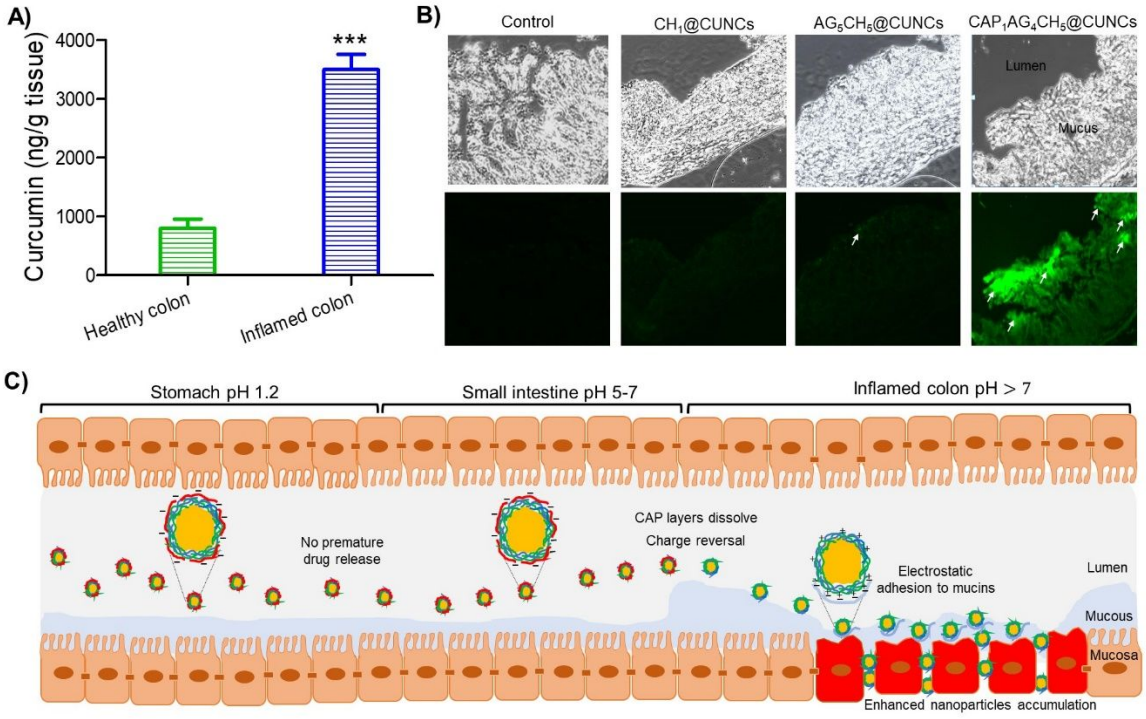

Figure 5. Accumulation of CH_1@CUNCs and core-shell nanoparticles in the inflamed colonic tissues of mice. (A) Quantitative analysis of curcumin accumulated in the healthy and inflamed colon samples from colitis mice after oral administration of $CAP_1AG_4CH_5$@CUNCs. (B) Confocal images showing the accumulation of CH_1@CUNCs and core-shell nanoparticles in inflamed colons of colitis mice. The fluorescent signals of core-shell nanoparticles are shown in green (white arrows). (C) Schematic illustration showing the adhesion and accumulation of

$CAP_1AG_4CH_5$@CUNCs in inflamed colons of colitis mice after oral administration. Data are represented as means ± SD ($n = 6$, *** $p < 0.001$ *versus* healthy colon).

Macroscopic grading of colitis

The DAI results indicating the severity of colitis in all studied mice groups are shown in Figure 6A. Mice in the healthy group showed constant DAI values throughout the study period, whereas increased DAI (up to 18 %) was recorded in the untreated colitis mice, indicating high colitis severity. Mice treated with CH_1@CUNCs and AG_5CH_5@CUNCs showed an increase in DAI by (~ 18 % and ~ 16 %, respectively), indicating high colitis severity. In contrast, mice treated with $CAP_1AG_4CH_5$@CUNCs showed significantly ($p < 0.001$) lower DAI than the untreated colitis mice, indicating a lower severity of colitis.

Further, the length of the colon in mice was measured to evaluate the severity of colitis at the end of the study (Figure 6B). The length of colon in mice in the healthy group was found to be ~ 9 cm. In mice treated with CH_1@CUNCs and AG_5CH_5@CUNCs, colon length was markedly shortened, similar to that in the colitis group (~ 5.2 and ~ 5.7 cm, respectively), indicating high colitis severity. In contrast, the colon length in mice treated with $CAP_1AG_4CH_5$@CUNCs, was found to be ~ 8.4 cm, which was significantly ($p < 0.01$) higher than that in untreated colitis mice, indicating low colitis severity in the $CAP_1AG_4CH_5$@CUNCs-treated group. Further, we recorded the spleen weight in mice as a macroscopic feature to analyze colitis severity (Figure 6C). An enlarged spleen is considered to be an important indicator of the extent of inflammation in colitis.[9] The spleen weight in healthy mice was ~ 0.083 ± 0.01 g, whereas, for untreated colitis mice it was ~ 0.221 ± 0.02 g, indicating severe colitis. The average spleen weight in $CAP_1AG_4CH_5$@CUNCs-

treated mice was ~ 0.107 ± 0.02 g, which was significantly ($p < 0.001$) lower than that of the untreated colitis mice. The spleen weight in CH_1@CUNCs and AG_5CH_5@CUNCs-treated mice was recorded to be 0.208 ± 0.01 g and 0.205 ± 0.02 g, respectively, which was similar to that in the untreated colitis mice. It is worth to noting that a suspension of free curcumin was also used to treat colitis mice as a separated study group. However, mice treated with free curcumin did not show any significant macroscopic improvement in colitis signs (lower DAI, shorter colon length and smaller spleen weight) as compared to untreated colitis mice (Figure S1).

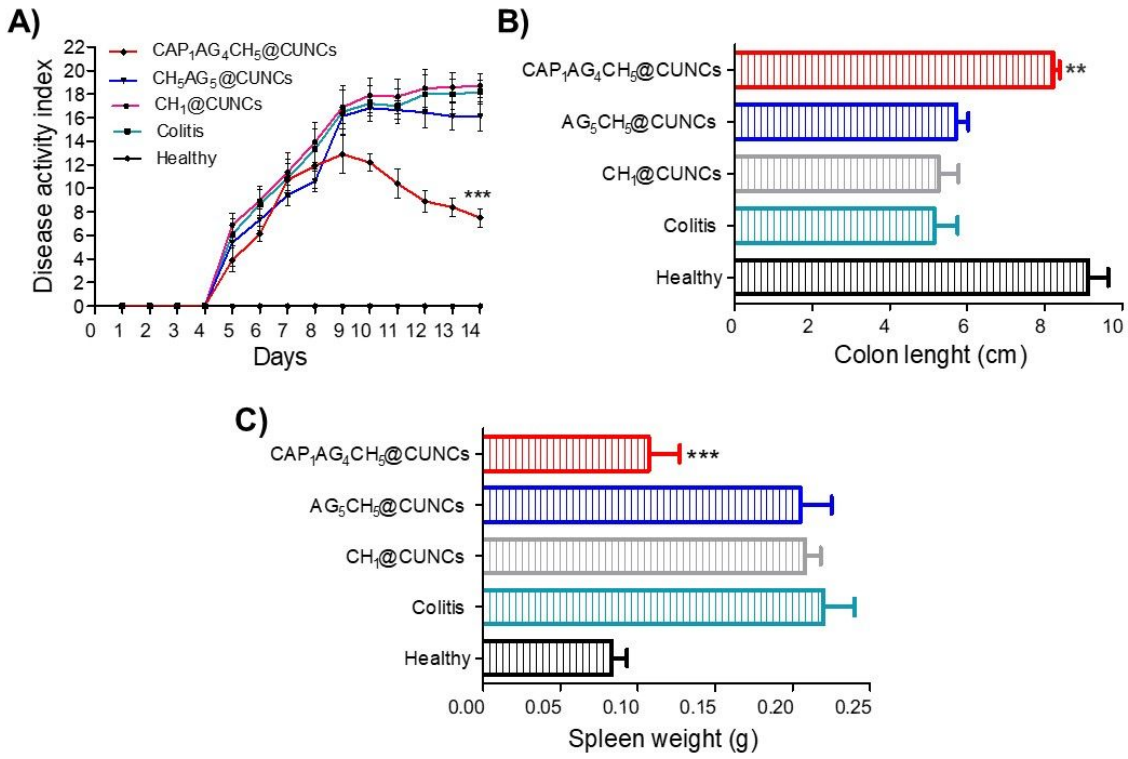

Figure 6. Macroscopic analysis of colitis in mice of all experimental groups. (A) Disease activity index. (B) Colon length. (C) Spleen weight. Data are presented as means ±SD ($n = 6$, ** $p < 0.01$ and *** $p < 0.001$ versus colitis group).

Histological analysis of colitis

The representative images of mice colon tissue sections stained with H&E from different treatment groups are shown in Figure 7A. The colon sections in healthy mice showed intact mucosa without any signs of mucosal inflammation, i.e., intact epithelium, absence of edema, and no infiltration of inflammatory cells, neutrophils, and macrophages. In contrast, the colonic sections of untreated colitis mice showed severe histological signs of mucosal inflammation, i.e., damaged epithelium, edema and infiltration of neutrophils and macrophages to the mucosa. Further, in mice treated with CH_1@CUNCs and AG_5CH_5@CUNCs, no pronounced improvements in the histological features of colitis were observed. As expected, the severe histological features of colitis were remarkably improved by treating mice with $CAP_1AG_4CH_5$@CUNCs. As shown in Figure 7A, re-epithelization of mucosa, absence of edema and low rate of neutrophil and macrophage infiltration to the mucosa were observed in mice treated with $CAP_1AG_4CH_5$@CUNCs. Mice treated with free curcumin did not significantly improve the histological features of colitis (Figure S2).

Immunofluorescence in mice colon

The representative images of colon sections stained for neutrophil and macrophage infiltrations using immunofluorescence are shown in Figure 7B and C, respectively. The colon sections from healthy mice showed no signs of neutrophil and macrophage infiltrations to the mucosa, indicating absence of colitis. However, in the colon sections from untreated colitis mice, neutrophil and macrophage infiltration to mucosa was observed, indicating severe colitis. The colon sections of

mice treated with CH_1@CUNCs and AG_5CH_5@CUNCs also showed increased neutrophil and macrophage infiltration, similar to that observed in untreated colitis mice. In contrast, treatment of mice with $CAP_1AG_4CH_5$@CUNCs, largely reduced the neutrophil and macrophage infiltration to mucosa, indicating improvement in severity of colitis. Free curcumin treatment did not significantly reduce the neutrophil and macrophage infiltration to mucosa as compared to untreated colitis mice (Figure S2).

Measurement of MPO activity and pro-inflammatory cytokine levels

MPO is considered as an important marker for detecting neutrophil infiltration to mucosa as well as degree of colitis severity.[43] Hence, we measured MPO activity in colon samples of all mice groups. The results indicated that all mice groups except the healthy mice exhibited variable MPO activities, indicating neutrophil infiltration. However, MPO activity was found to be significantly lower ($p < 0.001$) in the colon of mice treated with $CAP_1AG_4CH_5$@CUNCs than that in untreated colitis mice (Figure 7D).

We further confirmed the low neutrophil and macrophage infiltration in the colon samples of mice treated with $CAP_1AG_4CH_5$@CUNCs by determining TNF-α and IL-6 levels (Figure 7E and F). TNF-α and IL-6 are secreted by neutrophils and macrophages and two important inflammatory mediators associated with UC pathogenesis.[44] The levels of TNF-α and IL-6 in the colon samples were found to be increased in response to the induction of colitis in mice, whereas, they were shown to be significantly reduced ($p < 0.001$) after $CAP_1AG_4CH_5$@CUNCs treatment. The treatment with CH_1@CUNCs and AG_5CH_5@CUNCs did not result in any significant reduction in TNF-α and IL-6 levels when compared to that in untreated colitis mice (Figure 7E and F). Free

curcumin treatment did not significantly reduce the MPO activity and TNF-α and IL-6 concentrations as compared to untreated colitis mice (Figure S3).

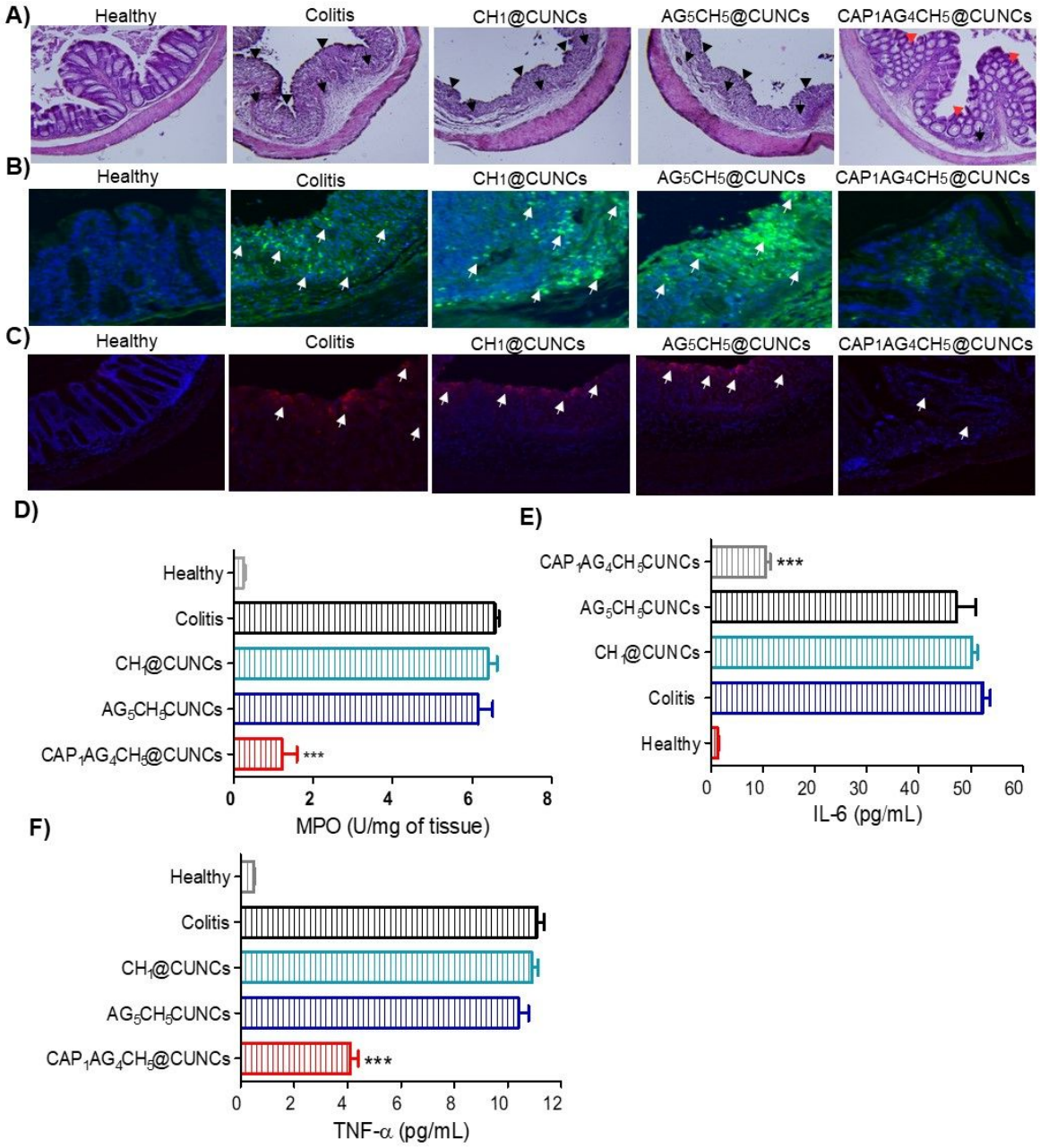

Figure 7. Histological analysis of colitis in mice of all experimental groups. (A) H&E-stained mice colon sections illustrate the histological changes of colitis (arrowheads, damaged epithelium;

black arrows, inflammatory cells; red arrows, re-epithelization). (B) Immunostained colon sections illustrate neutrophil infiltration into mucosa (white arrows). Green, neutrophils; Blue, DAPI for nuclear staining. (C) Immunostained colon sections illustrate macrophage infiltration into mucosa (white arrows). Red, macrophages (F4/80); Blue, DAPI for nuclear staining. (D) MPO activity in the colon samples. (E) IL-6 concentration in the colon samples. (F) TNF-α concentration in the colon samples. Data are presented as means ± SD ($n = 6$, *** $p < 0.001$ *versus* colitis group).

DISCUSSION

Core-shell nanoparticles were successfully prepared using an ultrasound-assisted antisolvent crystallization and LBL-coating techniques (Figure 1A).[27, 28] CH aqueous solution (antisolvent) was gradually added to curcumin in ethanol solution (solvent) and sonicated to fabricate drug nanocrystals and then coat with CH. Curcumin is a highly hydrophobic drug,[45] and tend to self-aggregate in the solution during the preparation of curcumin nanoparticles.[46] The aggregated nanocrystals do not represent suitable particle core for LBL-coating.[23] Hence, to prevent curcumin aggregation and prepare stable drug nanocrystals, important processing conditions and formulation parameters involved in the preparation were screened and optimized.[47] We found that using 2 mg/mL of CH aqueous solution as antisolvent with curcumin prepared in ethanol resulted in stable drug nanocrystals after sonication at 150 W/cm2 for 30 min. The drug nanocrystals (CH_1@CUNCs) were characterized for their particle size, PDI, surface charge and shape. The results showed that CH_1@CUNCs had an average size of 412 nm and positive surface charge of + 30 mV (Table. 1). Together, these results show that stable CH_1@CUNCs were produced and have suitable core for LBL-coating with the PE, CH and AG.

In UC therapy, a pH-sensitive polymer coating approach of nanoparticles showed early drug release by the nanoparticles in the upper GIT. This will result in reduced concentration of the drug available in colon, subsequently reducing the drug efficacy.[48, 49] In this study, we developed core-shell nanoparticle forms ($CAP_1AG_4CH_5$@CUNCs) that reduce the drug (curcumin) leakage in the upper GIT and delivers it specifically to the inflamed colon, thus decreasing the symptoms of experimental colitis in mice. To control curcumin leakage from $CAP_1AG_4CH_5$@CUNCs during their passage through the upper GIT, the CUNCs cores were coated with multiple layers of CH and AG followed by CAP. CH and AG are non-toxic biopolymers with good biodegradability and biocompatibility profiles. Both polymers have been widely used as carriers in colon-targeted nanoparticles.[50] CAP is a pH-sensitive polymer which is insoluble in the stomach pH while dissolving in the colonic pH. Hence, CAP was used as an enteric coating material to resist acid dissolution in the stomach and small intestine and deliver the drug to the colon.[51, 52] The bio-distribution and confocal microcopy imaging studies indicated that $CAP_1AG_4CH_5$@CUNCs were highly distributed in the colon than in the upper GIT tract after oral administration in mice.

Despite the significant advances in UC therapy, absence of nanoparticle accumulation in the inflamed tissues remains an issue. Recently, in our lab a new approach for enhancing the accumulation of nanoparticles in the inflamed colonic tissues was studied for UC therapy. This approach utilizes the pathophysiological changes occurring in the inflamed tissues, such as elevated levels of mucus production and mucosal disruption to promote higher accumulation of nanoparticles.[9] In our study, the quantitative analysis of curcumin concentration in colon samples confirmed significantly higher accumulation of $CAP_1AG_4CH_5$@CUNCs in the inflamed tissues than the healthy ones (Figure 5A). Moreover, the confocal microscopy images of colon samples showed enhanced accumulation of $CAP_1AG_4CH_5$@CUNCs into the inflamed colonic tissues

(Figure 5B). The higher accumulation could be attributed to the ability of $CAP_1AG_4CH_5$@CUNCs to maintain CUNCs cores without getting dissolved in the upper GIT. Further, upon reaching the colon, the nanoparticles get passively accumulated in the inflamed tissues by enhanced permeability and retention effect depending on their particle size.[9, 49, 53] Additionally the surface charge-reversing property of $CAP_1AG_4CH_5$@CUNCs (Figure 5C) further enhances their accumulation into the inflamed colons.

Curcumin, a major polyphenolic compound obtained from turmeric, has already been studied as an anti-inflammatory agent for the treatment of UC. It regulates the inflammatory responses by blocking the migration of innate immune cells, such as neutrophils and macrophages, from the peripheral circulation to mucosal inflammatory sites.[54, 55] Importantly, curcumin was recognized as a safe food additive by the US Food and Drug Administration.[56] However, when it was used orally in clinical trials, weak therapeutic effects were observed due to the inefficient drug delivery into the inflamed colon tissues.[45] A study by Xiao et al., has used micro/nanoparticle-drug delivery approach to overcome this issue in experimental murine colitis. However, the approach required high dose of curcumin (50 mg/kg/day) to treat colitis.[57] In our study, we proposed a simple and effective method of curcumin formulation using core-shell nanoparticles for the treatment of UC. Our results indicated that a lower dose of curcumin (15 mg/kg/day) is required to treat murine colitis, indicating enhanced drug potency. This is possible due to the colon-targeted delivery of $CAP_1AG_4CH_5$@CUNCs and its high accumulation into the inflamed tissues.

CONCLUSIONS

In this study, colon-targeted core-shell nanoparticles were developed using CUNCs as cores and pH-responsive polyelectrolyte multilayers of CH/AG/CAP as shells ($CAP_1AG_4CH_5$@CUNCs), which can specifically deliver the drug into the inflamed colon of UC. The *in vitro* release studies showed pH-dependent release of curcumin from $CAP_1AG_4CH_5$@CUNCs. In addition, the bio-distribution studies showed high colonic distribution of $CAP_1AG_4CH_5$@CUNCs in mice. Further, the quantitative analysis of the drug concentration in colonic tissues and confocal imagining of colons revealed that $CAP_1AG_4CH_5$@CUNCs were preferentially adhered and accumulated in inflamed colons rather than in healthy tissues. $CAP_1AG_4CH_5$@CUNCs showed enhanced therapeutic efficacy at treating DSS-induced colitis in mice. Overall, the drug delivery system developed in the current study has great potential for application in colon-targeted UC therapy.

SUPPORTING INFORMATION

Methodology on drug loading; Statistical analysis; Physicochemical characteristics of core-shell nanoparticles with shells having different numbers of CH/AG/CAP multilayers; Macroscopic analysis of colitis; Histological analysis of colitis and immunostaining of colonic tissues; MPO activity and pro-inflammatory cytokine levels

AUTHOR INFORMATION

Corresponding Author

Jin-Wook Yoo

College of Pharmacy, Pusan National University, Busandaehak-ro 63 beon-gil, Geumjeong-gu, Busan, South Korea.

Tel: +82-51-510-2807

Fax: +82 51 513 6754

E-mail: jinwook@pusan.ac.kr

NOTE

There is no conflict of interest to declare in this study.

ACKNOWLEDGMENTS

This research was supported by the Basic Science Research Program through the National Research Foundation of Korea (NRF) funded by the Ministry of Education (grant number: NRF-2019R1I1A3A01057849).

REFERENCES

1. Danese, S.; Fiocchi, C. Ulcerative colitis. *N. Engl. J. Med.* **2011,** 365, (18), 1713-1725.
2. Oshi, M. A.; Naeem, M.; Bae, J.; Kim, J.; Lee, J.; Hasan, N.; Kim, W.; Im, E.; Jung, Y.; Yoo, J.-W. Colon-targeted dexamethasone microcrystals with pH-sensitive chitosan/alginate/Eudragit S multilayers for the treatment of inflammatory bowel disease. *Carbohydr. Polym.* **2018,** 198, 434-442.
3. Kenyon, C. J.; Nardi, R. V.; Wong, D.; Hooper, G.; Wilding, I. R.; Friend, D. R. Colonic delivery of dexamethasone: a pharmacoscintigraphic evaluation. *Aliment. Pharmacol. Ther. Symp. Ser.* **1997,** 11, (1), 205-213.

4. Naeem, M.; Awan, U. A.; Subhan, F.; Cao, J.; Hlaing, S. P.; Lee, J.; Im, E.; Jung, Y.; Yoo, J.-W. Advances in colon-targeted nano-drug delivery systems: challenges and solutions. *Arch. Pharmacal Res.* **2020,** 43, (1), 153-169.
5. Zhang, M.; Merlin, D. Nanoparticle-based oral drug delivery systems targeting the colon for treatment of ulcerative colitis. *Inflammatory Bowel Dis.* **2018,** 24, (7), 1401-1415.
6. Thapaliya, R.; Shrestha, K.; Sharma, A.; Dhakal, N.; Manandhar, P.; Shrestha, S.; Bhattarai, R. Physicochemical characterization of naproxen microcrystals for colon specific pulsatile drug delivery designed using pulsincap technique. *J. Pharm. Invest.* **2019,** 49, (5), 553-564.
7. Kumar, J.; Newton, A. M. Rifaximin - chitosan nanoparticles for inflammatory bowel disease (IBD). *Recent Pat. Inflammation Allergy Drug Discovery* **2017,** 11, (1), 41-52.
8. Davoudi, Z.; Peroutka-Bigus, N.; Bellaire, B.; Wannemuehler, M.; Barrett, T. A.; Narasimhan, B.; Wang, Q. Intestinal organoids containing poly(lactic-co-glycolic acid) nanoparticles for the treatment of inflammatory bowel diseases. *J. Biomed. Mater. Res., Part A* **2018,** 106, (4), 876-886.
9. Naeem, M.; Oshi, M. A.; Kim, J.; Lee, J.; Cao, J.; Nurhasni, H.; Im, E.; Jung, Y.; Yoo, J.-W. pH-triggered surface charge-reversal nanoparticles alleviate experimental murine colitis via selective accumulation in inflamed colon regions. *Nanomed-nanotechnol.* **2018,** 14, (3), 823-834.
10. Ferri, D.; Gaviña, P.; Parra, M.; Costero, A. M.; El Haskouri, J.; Amorós, P.; Merino, V.; Teruel, A. H.; Sancenón, F.; Martínez-Máñez, R. Mesoporous silica microparticles

gated with a bulky azo derivative for the controlled release of dyes/drugs in colon. *R. Soc. Open Sci.* **2018,** 5, (8), 180873-180877.

11. Gupta, A. S.; Kshirsagar, S. J.; Bhalekar, M. R.; Saldanha, T. Design and development of liposomes for colon targeted drug delivery. *J. Drug Targeting* **2013,** 21, (2), 146-160.
12. Han, S.-M.; Na, Y.-G.; Lee, H.-S.; Son, G.-H.; Jeon, S.-H.; Bang, K.-H.; Kim, S.-J.; Lee, H.-J.; Cho, C.-W. Improvement of cellular uptake of hydrophilic molecule, calcein, formulated by liposome. *J. Pharm. Invest.* **2018,** 48, (5), 595-601.
13. Ma, Y.; Fuchs, A. V.; Boase, N. R. B.; Rolfe, B. E.; Coombes, A. G. A.; Thurecht, K. J. The in vivo fate of nanoparticles and nanoparticle-loaded microcapsules after oral administration in mice: Evaluation of their potential for colon-specific delivery. *Eur. J. Pharm. Biopharm.* **2015,** 94, 393-403.
14. Knipe, J. M.; Strong, L. E.; Peppas, N. A. Enzyme- and pH-responsive microencapsulated nanogels for oral delivery of sirna to induce TNF-alpha knockdown in the intestine. *Biomacromolecules* **2016,** 17, (3), 788-797.
15. Zhang, M.; Viennois, E.; Xu, C.; Merlin, D. Plant derived edible nanoparticles as a new therapeutic approach against diseases. *Tissue Barriers* **2016,** 4, (2), e1134415-e1134415.
16. Agarwal, A.; Lvov, Y.; Sawant, R.; Torchilin, V. Stable nanocolloids of poorly soluble drugs with high drug content prepared using the combination of sonication and layer-by-layer technology. *J. Controlled Release* **2008,** 128, (3), 255-260.

17. Rostami, M.; Zamani, R. M.; Aghajanzadeh, K. M.; Danafar, H. Sol–gel synthesis and characterization of zinc ferrite–graphene nano-hybrids for photo-catalytic degradation of the paracetamol. *J. Pharm. Invest.* **2018,** 48, (6), 657-664.
18. Sharma, S.; Verma, A.; Teja, B. V.; Shukla, P.; Mishra, P. R. Development of stabilized Paclitaxel nanocrystals: In-vitro and in-vivo efficacy studies. *Eur. J. Pharm. Sci.* **2015,** 69, 51-60.
19. Singh, D.; Bedi, N.; Tiwary, A. K. Enhancing solubility of poorly aqueous soluble drugs: critical appraisal of techniques. *J. Pharm. Invest*. **2018,** 48, (5), 509-526.
20. Kawabata, Y.; Wada, K.; Nakatani, M.; Yamada, S.; Onoue, S. Formulation design for poorly water-soluble drugs based on biopharmaceutics classification system: Basic approaches and practical applications. *Int. J. Pharm.* **2011,** 420, (1), 1-10.
21. Van Hoogevest, P.; Liu, X.; Fahr, A. Drug delivery strategies for poorly water-soluble drugs: the industrial perspective. *Expert Opin. Drug Delivery* **2011,** 8, (11), 1481-500.
22. Fuhrmann, K.; Polomska, A.; Aeberli, C.; Castagner, B.; Gauthier, M. A.; Leroux, J. C. Modular design of redox-responsive stabilizers for nanocrystals. *ACS Nano* **2013,** 7, (9), 8243-8250.
23. Polomska, A.; Gauthier, M. A.; Leroux, J. C. In vitro and in vivo evaluation of PEGylated layer-by-layer polyelectrolyte-coated paclitaxel nanocrystals. *Small* **2017,** 13, (2), 1-12.
24. Deshpande, S.; Sharma, S.; Koul, V.; Singh, N. Core–shell nanoparticles as an efficient, sustained, and triggered drug-delivery system. *ACS Omega* **2017,** 2, (10), 6455-6463.

25. Ghosh Chaudhuri, R.; Paria, S. Core/shell nanoparticles: classes, properties, synthesis mechanisms, characterization, and applications. *Chem. Rev.* **2011,** 112, (4), 2373-2433.
26. Wanawananon, K.; Moulton, S. E.; Wallace, G. G.; Liawruangrath, S. Fabrication of novel core–shell PLGA and alginate fiber for dual-drug delivery system. *Polym. Adv. Technol.* **2016,** 27, (8), 1014-1019.
27. Park, M.-W.; Yeo, S.-D. Antisolvent crystallization of roxithromycin and the effect of ultrasound. *Polym. Adv. Technol.* **2010,** 45, (10), 1402-1410.
28. Polomska, A.; Gauthier, M. A.; Leroux, J. C. In vitro and in vivo evaluation of PEGylated layer-by-layer polyelectrolyte-coated paclitaxel nanocrystals. *Small* **2017,** 13, (2), 1602066.
29. Chai, F.; Sun, L.; He, X.; Li, J.; Liu, Y.; Xiong, F.; Ge, L.; Webster, T. J.; Zheng, C. Doxorubicin-loaded poly (lactic-co-glycolic acid) nanoparticles coated with chitosan/alginate by layer by layer technology for antitumor applications. *Int. J. Nanomed.* **2017,** 12, 1791-1802.
30. Beloqui, A.; Coco, R.; Memvanga, P. B.; Ucakar, B.; des Rieux, A.; Preat, V. pH-sensitive nanoparticles for colonic delivery of curcumin in inflammatory bowel disease. *Int. J. Pharm.* **2014,** 473, (1-2), 203-212.
31. Cui, J.; Yu, B.; Zhao, Y.; Zhu, W.; Li, H.; Lou, H.; Zhai, G. Enhancement of oral absorption of curcumin by self-microemulsifying drug delivery systems. *Int. J. Pharm.* **2009,** 371, (1), 148-155.

32. Madhavi, M.; Madhavi, K.; Jithan, A. V. Preparation and in vitro/in vivo characterization of curcumin microspheres intended to treat colon cancer. *J. Pharm. BioAllied Sci.* **2012,** 4, (2), 164-171.
33. Zhang, J.; Liu, S.; Hu, X.; Xie, Z.; Jing, X. Cyanine-curcumin assembling nanoparticles for near-infrared imaging and photothermal therapy. *ACS Biomater. Sci. Eng.* **2016,** 2, (11), 1942-1950.
34. Cui, J.; Yu, B.; Zhao, Y.; Zhu, W.; Li, H.; Lou, H.; Zhai, G. Enhancement of oral absorption of curcumin by self-microemulsifying drug delivery systems. *Int. J. Pharm.* **2009,** 371, (1-2), 148-55.
35. Hartmann, G.; Bidlingmaier, C.; Siegmund, B.; Albrich, S.; Schulze, J.; Tschoep, K.; Eigler, A.; Lehr, H. A.; Endres, S. Specific type IV phosphodiesterase inhibitor rolipram mitigates experimental colitis in mice. *J. Pharmacol. Exp. Ther.* **2000,** 292, (1), 22-30.
36. Viennois, E.; Xiao, B.; Ayyadurai, S.; Wang, L.; Wang, P. G.; Zhang, Q.; Chen, Y.; Merlin, D. Micheliolide, a new sesquiterpene lactone that inhibits intestinal inflammation and colitis-associated cancer. *Lab. Invest.* **2014,** 94, 950.
37. Weigmann, B.; Lehr, H. A.; Yancopoulos, G.; Valenzuela, D.; Murphy, A.; Stevens, S.; Schmidt, J.; Galle, P. R.; Rose-John, S.; Neurath, M. F. The transcription factor NFATc2 controls IL-6-dependent T cell activation in experimental colitis. *J. Exp. Med.* **2008,** 205, (9), 2099-2110.
38. Naeem, M.; Bae, J.; Oshi, M. A.; Kim, M.-s.; Moon, H. R.; Lee, B. L.; Im, E.; Jung, Y.; Yoo, J.-W. Colon-targeted delivery of cyclosporine A using dual-functional Eudragit®

FS30D/PLGA nanoparticles ameliorates murine experimental colitis. *Int. J. Nanomed.* **2018,** 13, 1225-1230.

39. Kim, J. J.; Shajib, M. S.; Manocha, M. M.; Khan, W. I. Investigating intestinal inflammation in DSS-induced model of IBD. *J. Visualized Exp.* **2012**, (60), 3678
40. Wan, S.; Sun, Y.; Qi, X.; Tan, F. Improved bioavailability of poorly water-soluble drug curcumin in cellulose acetate solid dispersion. *AAPS PharmSciTech* **2012,** 13, (1), 159-166.
41. Park, S. C.; Kim, M. J.; Choi, K.; Kim, J.; Choi, S.-O. Influence of shell compositions of solution blown PVP/PCL core–shell fibers on drug release and cell growth. *RSC Adv.* **2018,** 8, (57), 32470-32480.
42. Santos, A. C.; Pattekari, P.; Jesus, S.; Veiga, F.; Lvov, Y.; Ribeiro, A. J. Sonication-assisted layer-by-layer assembly for low solubility drug nanoformulation. *ACS Appl. Mater. Interfaces* **2015,** 7, (22), 11972-11983.
43. Mendoza, J. L.; Abreu, M. T. Biological markers in inflammatory bowel disease: Practical consideration for clinicians. *Gastroenterol. Clin. Biol.* **2009,** 33, (Supplement 3), S158-S173.
44. Poh, S.; Lin, J. B.; Panitch, A. Release of anti-inflammatory peptides from thermosensitive nanoparticles with degradable cross-links suppresses pro-inflammatory cytokine production. *Biomacromolecules* **2015,** 16, (4), 1191-1200.
45. Anand, P.; Kunnumakkara, A. B.; Newman, R. A.; Aggarwal, B. B. Bioavailability of curcumin: problems and promises. *Mol. Pharmaceutics* **2007,** 4, (6), 807-818.

46. Moorthi, C.; Krishnan, K.; Manavalan, R.; Kathiresan, K. Preparation and characterization of curcumin-piperine dual drug loaded nanoparticles. *Asian Pac. J. Trop. Biomed.* **2012,** 2, (11), 841-848.

47. Iurian, S.; TomuŢA, I.; Rus, L.; Achim, M.; Leucuta, S. E. Optimization of the sonication process for meloxicam nanocrystals preparation. *Clujul Med.* **2015,** 88, (3), 366-372.

48. Lamprecht, A.; Ubrich, N.; Yamamoto, H.; Schäfer, U.; Takeuchi, H.; Lehr, C.-M.; Maincent, P.; Kawashima, Y. J. Design of rolipram-loaded nanoparticles: comparison of two preparation methods. *J. Controlled Release* **2001,** 71, (3), 297-306.

49. Lamprecht, A.; Ubrich, N.; Yamamoto, H.; Schäfer, U.; Takeuchi, H.; Maincent, P.; Kawashima, Y.; Lehr, C.-M. Biodegradable nanoparticles for targeted drug delivery in treatment of inflammatory bowel disease. *J. Pharmacol. Exp. Ther.* **2001,** 299, (2), 775-781.

50. Chourasia, M. K; Jain, S. K. Polysaccharides for colon targeted drug delivery. *Drug Delivery* **2004,** 11, (2), 129-148.

51. Ganguly, K.; Aminabhavi, T. M.; Kulkarni, A. R. Colon targeting of 5-fluorouracil using polyethylene glycol cross-linked chitosan microspheres enteric coated with cellulose acetate phthalate. *Ind. Eng. Chem. Res.* **2011,** 50, (21), 11797-11807.

52. Levine, D. S.; Raisys, V. A.; Ainardi, V. Coating of oral beclomethasone dipropionate capsules with cellulose acetate phthalate enhances delivery of topically active antiinflammatory drug to the terminal ileum. *Gastroenterology* **1987,** 92, (4), 1037-1044.

53. Lamprecht, A.; Schafer, U.; Lehr, C. M. Size-dependent bioadhesion of micro- and nanoparticulate carriers to the inflamed colonic mucosa. *Pharm. Res.* **2001,** 18, (6), 788-793.

54. Ukil, A.; Maity, S.; Karmakar, S.; Datta, N.; Vedasiromoni, J. R.; Das, P. K. Curcumin, the major component of food flavour turmeric, reduces mucosal injury in trinitrobenzene sulphonic acid-induced colitis. *Br. J. Pharmacol.* **2003,** 139, (2), 209-218.

55. Young, N. A.; Bruss, M. S.; Gardner, M.; Willis, W. L.; Mo, X.; Valiente, G. R.; Cao, Y.; Liu, Z.; Jarjour, W. N.; Wu, L. C. Oral administration of nano-emulsion curcumin in mice suppresses inflammatory-induced NFkappaB signaling and macrophage migration. *PloS one* **2014,** 9, (11), e111559.

56. Clinical development plan: curcumin. *J. Cell. Biochem. Suppl.* **1996,** 26, 72-85.

57. Xiao, B.; Si, X.; Zhang, M.; Merlin, D. Oral administration of pH-sensitive curcumin-loaded microparticles for ulcerative colitis therapy. *Colloids Surf., B* **2015,** 135, 379-385.

Table of contents graphic (TOC)